

DESERT DUST EFFECTS IN THE RESULTS OF ATMOSPHERIC CORRECTION OF SATELLITE SEA COLOR OBSERVATIONS

V.V. Suslin, V.S. Suetin, S.N. Korolev, A.A. Kucheryavyi

Marine Hydrophysical Institute, National Academy of Sciences of Ukraine, 2 Kapitanskaya str., Sevastopol, Ukraine,
e-mail: otdp@alpha.mhi.iuf.net

The space-borne ocean color instruments SeaWiFS and MODIS measure the spectrum of sunlight reflected from the ocean-atmosphere system at several visible and near-infrared wavebands. These radiance spectra are used to estimate the spectra of water-leaving radiance (sea color) through the atmospheric correction procedure [1]. Unfortunately, in the Black Sea and the Mediterranean areas, due to errors in atmospheric correction, possibilities of determination of full spectra of water-leaving radiance are very limited. The matter consists in very complicated atmospheric effects, which should be accurately accounted for in the processing of satellite observations [2-4].

Optical properties of atmospheric aerosol in the considered region demonstrate very strong diversity and often do not satisfy the assumptions which are used in the standard NASA's atmospheric correction algorithm. In particular, due to absorption effects, desert dust has lower aerosol radiance at the shorter wavelengths than any of that models, and can not be accounted for adequately [1, 5]. This problem was recently considered in many papers, for example see [6, 7]. The general approach is based on the joint modeling the optical properties of sea water and atmospheric aerosol. Such ways are applicable for Case 1 ocean waters only, but in the Black Sea, water does not belong to Case 1 type. So, we need to look for the different logic of the remote-sensing data interpretation. For this aim, it is helpful to consider the satellite data together with *in situ* Aeronet determinations of aerosol properties [8, 9].

We suppose that some strong atmospheric effects are similar in the Black Sea and the Mediterranean regions, and one type of them is determined by desert dust. Thus, the detailed study of dust in the Mediterranean area will be helpful for the interpretation of satellite observations of the Black Sea as well. Considering the satellite true-color BROWSE images from NASA GSFC archive [10], one often can clearly see dust plumes in the form of more or less homogeneous large clouds. These dust clouds usually have the different hue and lightness in respect to ordinary atmospheric clouds. When such plume covers the Aeronet site, it is possible to obtain the additional confirmation that there really dust occurs.

Fig. 1 presents the example of the pronounced short term temporal variability of aerosol optical thickness, $\tau_A(870)$, at the wavelength λ of 870 nm, during 17 days in 2003 according to the data of Aeronet site "Forth Crete" (situated at the north coast of the Crete island). Two peaks with the values of $\tau_A(870)$ up to 0.4 – 0.5 observed near August 31 – September 1 (Julian days 243 – 244) and September 9 – 10 (Julian days 252 – 253) signify short-lived intense dust storms. These variations of $\tau_A(870)$ are accompanied by dramatic changes of Angstrom coefficient α from 1.0 – 2.0 outside the dust events down to 0.2 – 0.5 for the days when $\tau_A(870)$ reaches maxima. Unfortunately, for the considered time interval, there is no Level-2.0 data of single scattering albedo ω_0 for the situations with low $\tau_A(870)$ in the Aeronet archive (reprocessed in autumn 2006). Therefore, it is difficult to determine definitely what type of aerosol took place there. But on the other hand, the values of ω_0 exist for that days, when dust events occurred, and these values exhibit wavelength dependence from $\omega_0 = 0.88 - 0.90$ at $\lambda = 441$ nm to $\omega_0 = 0.96 - 0.97$ at $\lambda = 870$ nm. It is in good agreement with well-known property of dust aerosol – ω_0 has higher values at longer wavelengths due to the increased contribution of scattering from coarse particle mode [11].

To analyse the resulting distortions in L_{WN} spectra, we considered the satellite data collected in the sets of successive days with very different atmospheric conditions.

This approach is illustrated by the detailed analysis of the data which correspond to the local peak for 9 – 10 September, 2003 (Julian days 252-253) in Fig. 1. The true color SeaWiFS image of September 9, 2003 (not shown here) displays dust cloud, which covers a vast space over and around the

Crete island. The density of this dust cloud is not uniform on the square. In the close vicinity of the Crete island it is so high, that the standard Level-2 satellite data processing products such as normalized water-leaving radiances L_{WN} , τ_A , and α were not generated for this area. At the same time, there is the extensive transitional zone eastward of Crete, where dust density is not so high, and the SeaWiFS data were not excluded from the processing. This feature is rather typical for desert dust events, and our attention is focused on the analysis of such transitional zones. In the considered time interval, it is essential that the sky was very clear on September, 8 almost over the whole eastern part of the Mediterranean Sea. Fig. 2a shows the comparison between the values of $L_{WN}(443)$ for two days: September 8 and 9, 2003. For plotting this figure, the standard SeaWiFS data were used, selected within the narrow bar (section, 0.05° wide on latitude) between 29.5°E and 32.5°E . This section crosses the edge of the dust plume, observed here on September 9, at nearly normal direction. Because the atmosphere was very clear on September 8, the values of $L_{WN}(443)$ were rather high about $1.8 \text{ mW} \cdot \text{cm}^{-2} \cdot \mu \text{m}^{-1} \cdot \text{sr}^{-1}$ and stable. In the eastern part of the section, the atmosphere was clear on September 9 as well (see Fig. 2b), and thus for this day $L_{WN}(443)$ has nearly the same value. In Fig. 2b, the values of satellite-derived $\tau_A(865)$, obtained for September 9, vary from ≈ 0.08 up to ≈ 0.28 , and corresponding values of $L_{WN}(443)$ also vary in the interval from ≈ 1.8 down to $\approx 1.2 \text{ mW} \cdot \text{cm}^{-2} \cdot \mu \text{m}^{-1} \cdot \text{sr}^{-1}$ with negative correlation in respect to $\tau_A(865)$.

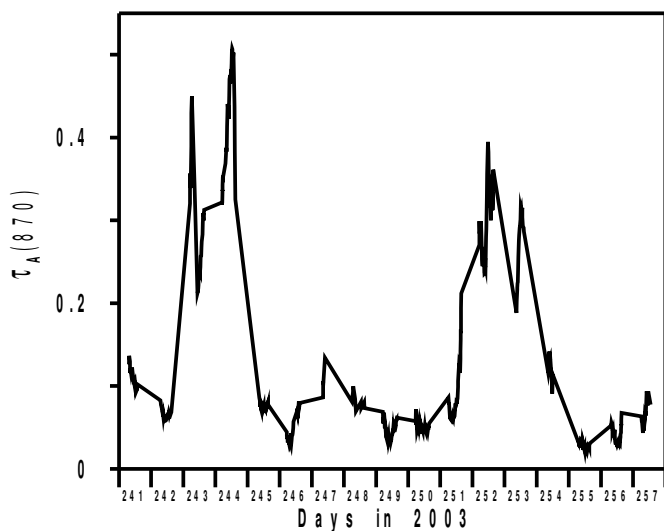


Fig. 1. Time series plot for the aerosol optical thickness, $\tau_A(870)$, between August 29 (Julian day 241) and September 14, 2003 (Julian day 257) in Aeronet site "Forth Crete".

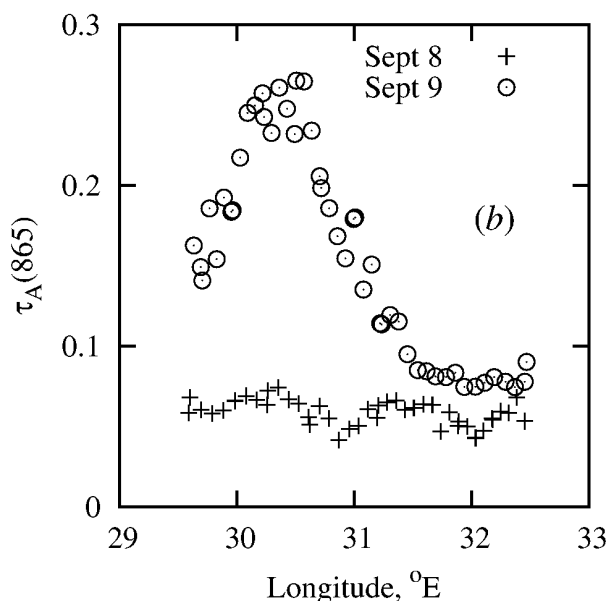
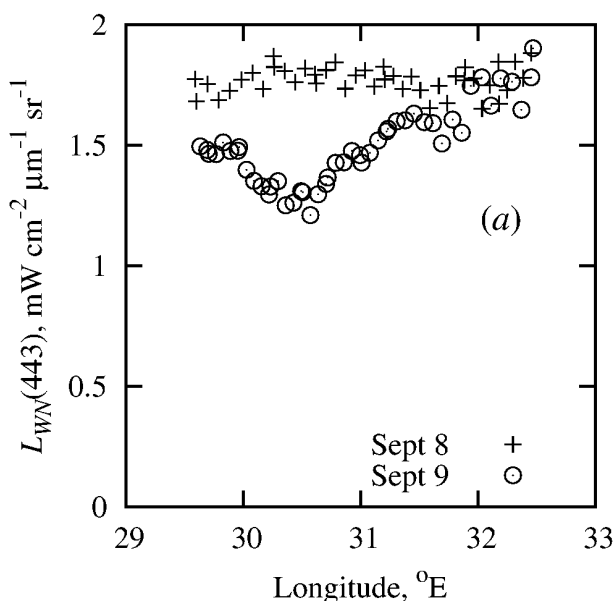


Fig. 2. Spatial variations of satellite-derived values of $L_{WN}(443)$ – (a), and $\tau_A(865)$ – (b), along the linear section in the Eastern Mediterranean Sea near 34.64°N, for two days in September 2003; the dates of satellite measurements are indicated in the legends.

The most essential distortions in $L_{WN}(\lambda)$ values are revealed just in such transitional zones at the edges of dust plumes, because the satellite data are completely discarded in the processing procedure together with ordinary atmospheric clouds, if the dust density is too high.

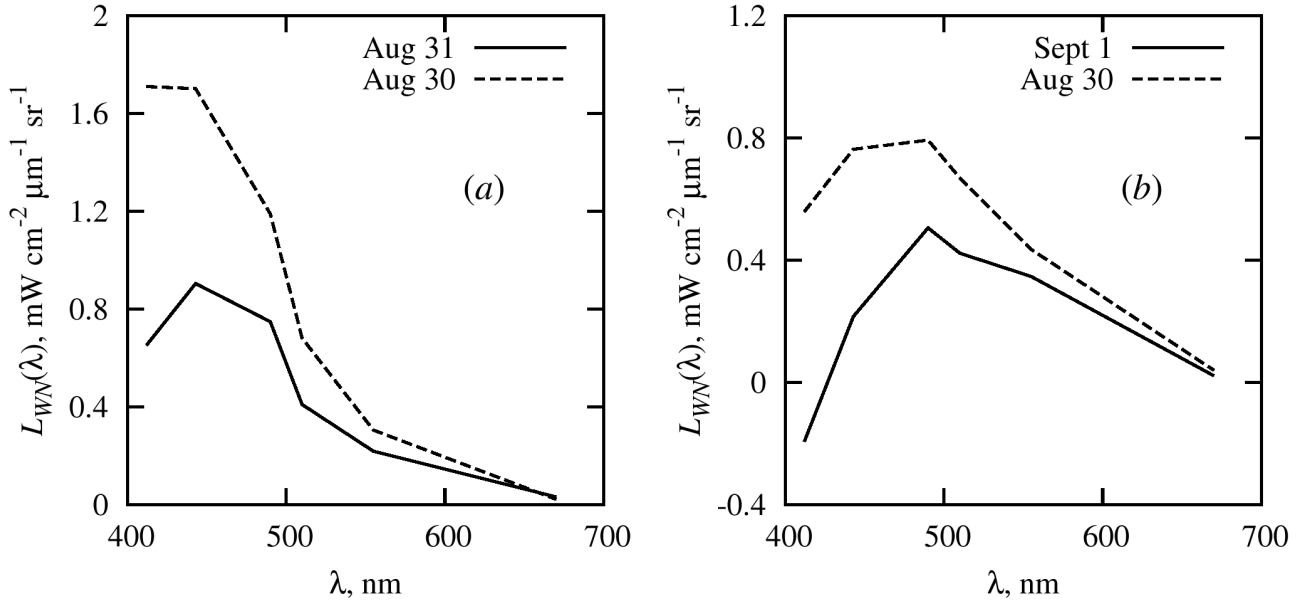


Fig. 3. Comparison of typical satellite-derived spectra of $L_{WN}(\lambda)$ in two selected sites: (a) – Mediterranean Sea (near the Crete island) on 30 and 31 August 2003, and (b) – Black Sea (north-east part) on 30 August and 1 September 2003; the dates of satellite measurements are indicated in the legends.

The dust aerosol effect consists in the underestimation of the standard satellite-derived $L_{WN}(\lambda)$ spectra in the visible domain, and this effect is more essential for shorter wavelengths. Fig. 3a shows the example of comparison between the SeaWiFS-derived $L_{WN}(\lambda)$ spectra for two days in the Mediterranean Sea near the north coast of the Crete island, not far from Aeronet site "Forth Crete". According to Fig. 1 and the analysis of the series of true color satellite images the atmosphere was rather clear on August 30, and after that – on August 31, the dust cloud already took place in the considered region. Fortunately, the standard Level-2 values of $L_{WN}(\lambda)$ were derived from SeaWiFS measurements in this dust cloud. It is easy to see the large difference between these two spectra, especially for $\lambda < 500$ nm. For instance, the $L_{WN}(443)$ value decreases from 1.9 to 0.8 $\text{mW} \cdot \text{cm}^{-2} \cdot \mu\text{m}^{-1} \cdot \text{sr}^{-1}$ when $\tau_A(870)$ increases from ≈ 0.05 to ≈ 0.5 (see Fig. 1). In summary, when dust events occur, the negative spatial (Figs. 2) and temporal (Figs. 1 and 3a) correlation between L_{WN} and τ_A exists. We analyzed many similar data sets for the Mediterranean region and obtained a lot of analogous results. This provides the possibility to explain similar distortions in $L_{WN}(\lambda)$ spectra, which often are observed in the Black Sea [2, 12]. Fig. 3b presents the indicative example for this and shows standard Level-2 SeaWiFS spectra of $L_{WN}(\lambda)$ in the north-eastern part of the Black Sea on 30 August and 1 September, 2003. Here, the most interesting feature is that for dusty conditions (on September 1) $L_{WN}(412)$ has negative value, while two days before (on August 30) it had essentially different value. This is likely the result of just the same dust event, which was observed near the Crete island on 31 August.

In principle, if to analyse the time series of satellite images, it is possible to reveal the presence of the dust aerosol from the spectra of $L_{WN}(\lambda)$ and satellite-derived fields of aerosol optical thickness and

Angstrom coefficient without use of supporting *in situ* Aeronet information. The corresponding strongly erroneous data should be discarded from the practical utilization.

Acknowledgements. The authors are grateful to Ocean Biology Processing Group (Code 614.2), NASA Goddard Space Flight Center, for providing the satellite data. Also, the AERONET project is thanked, and the contribution of E. Drakakis, PI of the 'FORTH_CRETE' Aeronet site, is gratefully acknowledged.

References

1. Gordon, H.R. Atmospheric correction of ocean color imagery in the Earth Observing System era // J.Geophys. Res. 1997. V. 102, No. D14. P. 17081–17106.
2. Suetin, V.S., Korolev, S.N., Suslin, V.V., Kucheryavyi, A.A. Manifestation of atmospheric distortions in the SeaWiFS data in the vicinity of the oceanographic platform in Katsiveli in the summer 2002 // Ecological safety of coastal and shelf zones and complex use of shelf resources. 2004. No.11. P. 174–183 (*in Russian*).
3. Suetin, V. S., Suslin, V. V., Kucheryavyi, A. A., et al. Peculiarities of data interpretation of the Black Sea remote optical observations by SeaWiFS // Mar. Hydrophys. Journal. 2001. No. 2. P. 71–80 (*in Russian*).
4. Suslin, V.V., Suetin, V.S., Korolev, S.N., Kucheryavyi, A.A. Possibilities of the Black Sea bio–optical characteristics estimation from SeaWiFS data. Proc. 1st Int. Conf. “Current Problems in Optics of Natural Waters (ONW’2001)”. St.Petersburg, 2001. P. 222–227.
5. Bailey, S. W., Werdell, P. J. A multi-sensor approach for the on-orbit validation of ocean color satellite data products // Remote Sens. Environ. 2006. V. 102. P. 12–23.
6. Nobileau, D., Antoine, D. Detection of blue-absorbing aerosols using near infrared and visible (ocean color) remote sensing observations // Remote Sens. Environ. 2005. V. 95. P. 368–387.
7. Moulin, C., Gordon, H. R., Banzon, V. F., Evans, R. H. Assessment of Saharan dust absorption in the visible from SeaWiFS imagery // J.Geophys. Res. 2001. V. 106. P. 18239–18249.
8. Holben, B.N., et al. AERONET – A federated instrument network and data archive for aerosol characterization // Remote Sens. Environ. 1998. V. 66. P. 1–16.
9. <http://aeronet.gsfc.nasa.gov/>
10. <http://oceancolor.gsfc.nasa.gov/>
11. Dubovik, O., Holben, B. N., Eck, T. F., et al. Variability of absorption and optical properties of key aerosol types observed in worldwide locations // J. Atmos. Sci. 2002. V.59. P. 590– 608.
12. Suetin, V.S., Korolev, S.N., Suslin, V.V., Kucheryavyi, A.A. Making more accurate interpretation of the Black Sea satellite observations provided by SeaWiFS in the autumn 1998 // Mar. Hydrophys. Journal. 2007 (*accepted, in Russian*).